

Electronic Structure of Perovskites: Lessons from Hybrid Functionals

Cesare Franchini

University of Vienna, Computational Materials Physics

cesare.franchini@univie.ac.at

September 21, 2015

Outline

① Intro: Perovskites

② Computational Modeling

- The Many Body Hamiltonian
- HF & DFT
- Hybrid Functionals

③ Results: Hybrid Functionals applied to Perovskites

- The 3d LaMO_3 perovskite dataset
- 4d and 5d perovskites (RTcO_3 & BaIrO_3)
- Metal-to-insulator (MIT) transition in LaMnO_3
- MIT and polarons in BaBiO_3
- Multiferroicity in PbNiO_3
- Crystal Structure Prediction: SrPbO_3

Once Upon a Time in the Ural Mountains

In 1839, the Prussian mineralogist Gustav Rose discovered a new mineral, CaTiO_3 , which he named perovskite, in honor of the Russian mineralogist Count Lev A. Perovski.



Gustav Rose



CaTiO_3



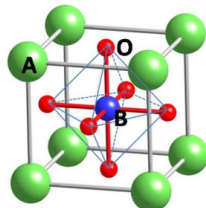
Lev A. Perovski

Once Upon a Time in the Ural Mountains

In 1839, the Prussian mineralogist Gustav Rose discovered a new mineral, CaTiO_3 , which he named **perovskite**, in honor of the Russian mineralogist Count Lev A. Perovski.



Gustav Rose



ABO_3



Lev A. Perovski

Basics: Chemistry

- $A^{2+}B^{4+}O_3^{2-}$: high chemical flexibility

A-site ion: large cation

Alkaline earth metal → Ca, Sr, Ba

Rare earth element → La, Sc, Y

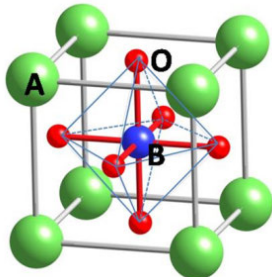
B-site ion: transition metal (TM) elements

3d → Ti, V, Mn, Fe, Co, Ni, Cu

4d → Nb, Tc, Ru, Rh

5d → Os, Ir

C-site ion: Oxygen



* Lanthanide series

** Actinide series

Basics: Chemistry

- $A^{2+}B^{4+}O_3^{2-}$: high chemical flexibility

A-site ion: large cation

Alkaline earth metal → Ca, Sr, Ba

Rare earth element → La, Sc, Y

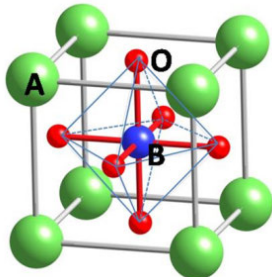
B-site ion: transition metal (TM) elements

3d → Ti, V, Mn, Fe, Co, Ni, Cu

4d → Nb, Tc, Ru, Rh

5d → Os, Ir

C-site ion: Oxygen



* Lanthanide series

** Actinide series

Basics: Chemistry

- $A^{2+}B^{4+}O_3^{2-}$: high chemical flexibility

A-site ion: large cation

Alkaline earth metal → Ca, Sr, Ba

Rare earth element → La, Sc, Y

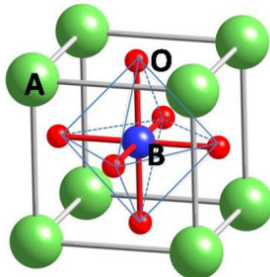
B-site ion: transition metal (TM) elements

$3d \rightarrow$ Ti, V, Mn, Fe, Co, Ni, Cu

$4d \rightarrow$ Nb, Tc, Ru, Rh

$5d \rightarrow$ Os, Ir

C-site ion: Oxygen

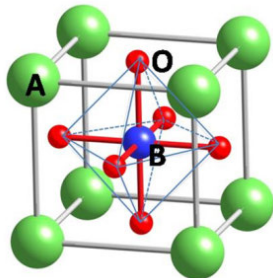


Financial ratios

$\beta\beta$ -Actinide series

La	Ce	Pr	Nd	Pm	Sm	Eu	Gd	Tb	Dy	Ho	Er	Tm	Yb
Ac	Th	Pa	U	Np	Pu	Am	Cm	Bk	Cf	Es	Fm	Md	No

Basics: Structure



- Goldschmidt tolerance factor t

$$t = (R_A + R_O)/\sqrt{2}(R_B + R_O)$$

$t=1$

Cubic ($R_A = R_B$)

SrTiO_3

$t > 1$

Hexagonal ($R_A > R_B$)
face-sharing of octahedra

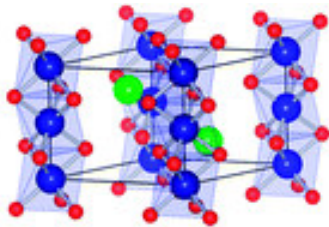
$t = 0.71 - 0.9$

Orthorhombic ($R_A < R_B$)
Rhombohedral

$t > 0.71$

Different structures ($R_A \sim R_B$)

Basics: Structure



Fuks et al., J. Mater. Chem. A 1 14320 (2013)

- Goldschmidt tolerance factor t

$$t = (R_A + R_O)/\sqrt{2}(R_B + R_O)$$

$$t = 1$$

$$t > 1$$

Cubic ($R_A = R_B$)

Hexagonal ($R_A > R_B$)

face-sharing of octahedra

$(\text{Ba},\text{Sr})(\text{Co},\text{Fe})\text{O}_3$, BaNiO_3

Orthorhombic ($R_A < R_B$)

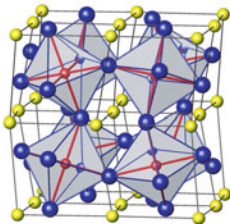
Rhombohedral

Different structures ($R_A \sim R_B$)

$$t = 0.71 - 0.9$$

$$t > 0.71$$

Basics: Structure



Pavarini *et al.*, New J. Phys. 7, 188 (2005)

- Goldschmidt tolerance factor t

$$t = (R_A + R_O)/\sqrt{2}(R_B + R_O)$$

$$t = 1$$

Cubic ($R_A = R_B$)

$$t > 1$$

Hexagonal ($R_A > R_B$)

face-sharing of octahedra

$$t = 0.71 - 0.9$$

Orthorhombic ($R_A < R_B$)

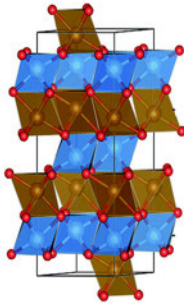
Rhombohedral

GdFeO_3

$$t > 0.71$$

Different structures ($R_A \sim R_B$)

Basics: Structure



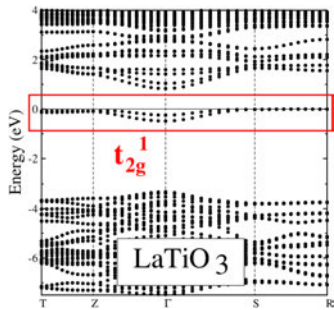
- Goldschmidt tolerance factor t

$$t = (R_A + R_O)/\sqrt{2}(R_B + R_O)$$

$t = 1$	Cubic ($R_A = R_B$)
$t > 1$	Hexagonal ($R_A > R_B$) face-sharing of octahedra
$t = 0.71 - 0.9$	Orthorhombic ($R_A < R_B$) Rhombohedral
$t > 0.71$	Different structures ($R_A \sim R_B$) Ilmenite FeTiO_3

Ribeiro *et al.*, RSC Adv., 4, 59839 (2014)

Basics: TM electron shell



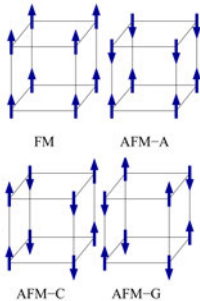
- Electrons: partially filled (3)d states

Electron localization (narrow bands, W)

Strong Coulomb correlations (U)

$U/W \rightarrow$ Mott–Hubbard insulator

Basics: TM electron shell



- Electrons: partially filled $(3)d$ states

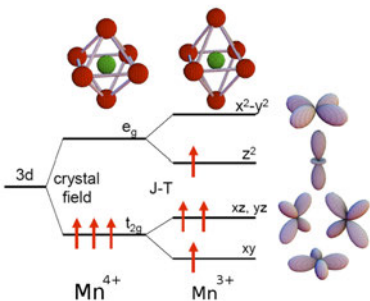
Electron localization (narrow bands, W)

Strong Coulomb correlations (U)

$U/W \rightarrow$ Mott–Hubbard insulator

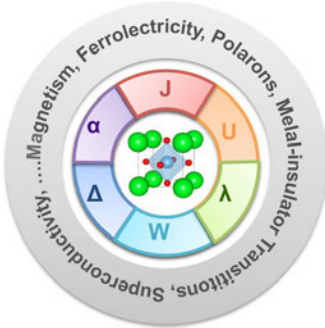
Different types of magnetic orderings

Basics: TM electron shell



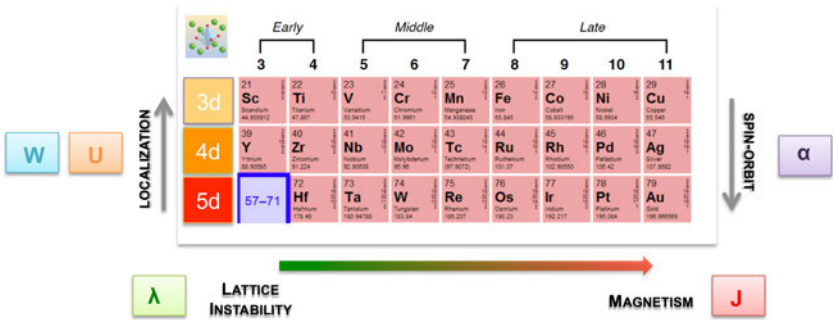
- Electrons: partially filled ($3d$) states
 - Electron localization (narrow bands, W)
 - Strong Coulomb correlations (U)
 - $U/W \rightarrow$ Mott–Hubbard insulator
 - Different types of magnetic orderings
- Jahn-Teller distortions** in e_g band perovskites (electron-phonon interaction)

Basics: Many (tunable) competing interactions



- W Bandwidth
- Δ Crystal Field
- α Spin-orbit
- J Hund's coupling
- U e-e repulsion
- λ e-ph interaction

Basics: Many (tunable) competing interactions



Competing and tunable energy scales give rise to a variety of functionalities

Basics: Applications

Wide spectrum of attractive properties \Rightarrow large variety of functional behavior...

Property	Application	Material	Catalytic	Catalyst	LaFeO ₃ , La(Ce,Co)O ₃
	SOFC electrolyte			Multilayer capacitor	
Proton conductivity	Hydrogen sensor	BaCeO ₃ , SrCeO ₃ BaZrO ₃	Electrical/ dielectric	Dielectric resonator	BaTiO ₃ , BaZrO ₃
	H ₂ production/ extraction			Thin film resistor	
Ionic conductivity	Solid electrolyte	(La,Sr)(Ga,Mg)O _{3-δ}		Magnetic memory	GdFeO ₃ , LaMnO ₃
Mixed conductivity	SOFC electrode	La(Sr,Ca)MnO _{3-δ} LaCoO ₃ (La,Sr)(Co,Fe)O _{3-δ}		Ferromagnetism	
	Piezoelectric transducer	BaTiO ₃ , Pb(Zr,Ti)O ₃	Optical	Electrooptical modulator	(Pb,La)(Zr,Ti)O ₃
Ferroelectric/ piezoelectric	Thermistor, actuator	Pb(Mg,Nb)O ₃		Laser	YAlO ₃ , KNbO ₃
			Super- conductivity	Superconductor	Ba(Pb,Bi)O ₃ , BaKBiO ₃

Basics: Applications

...and new emerging phenomena

- Oxide electronics: Two dimensional electron gas @ perovskite interface ($\text{SrTiO}_3\|\text{LaAlO}_3$) and surface (SrTiO_3)
- Spintronics: half-metallic double perovskites
- Photovoltaics: Perovskite solar cells (Halide perovskites, $\text{CH}_3\text{NH}_3\text{PbX}_3$)

Computational Modeling

Realistic modeling of perovskites very challenging: the state of each electron **strongly** depends on the state of the other electrons of the system, which are coupled (or **correlate** with each other) via the Coulomb interaction.

Computational Modeling

Realistic modeling of perovskites very challenging: the state of each electron **strongly** depends on the state of the other electrons of the system, which are coupled (or **correlate** with each other) via the Coulomb interaction.

At the core of the problem there is the solution of the many body Hamiltonian.

Basic Hamiltonian of a system of N electrons and M nuclei

$$\begin{aligned}\hat{H} = & -\frac{\hbar^2}{2m_e} \sum_{i=1}^N \nabla_i^2 - \sum_{n=1}^M \frac{\hbar^2}{2M_n} \nabla_n^2 + \frac{1}{4\pi\epsilon_0} \frac{1}{2} \sum_{i,j=1; i \neq j}^N \frac{e^2}{|\mathbf{r}_i - \mathbf{r}_j|} \\ & - \frac{1}{4\pi\epsilon_0} \sum_n^M \sum_i^N \frac{Z_n e^2}{|\mathbf{r}_i - \mathbf{R}_n|} + \frac{1}{4\pi\epsilon_0} \frac{1}{2} \sum_{n,m=1; n \neq m}^M \frac{Z_n Z_m e^2}{|\mathbf{R}_n - \mathbf{R}_m|}\end{aligned}$$

The Many Body Hamiltonian

Basic Hamiltonian of a system of N electrons and M nuclei

$$\begin{aligned}\hat{H} = & -\frac{\hbar^2}{2m_e} \sum_{i=1}^N \nabla_i^2 - \sum_{n=1}^M \frac{\hbar^2}{2M_n} \nabla_n^2 + \frac{1}{4\pi\epsilon_0} \frac{1}{2} \sum_{i,j=1; i \neq j}^N \frac{e^2}{|\mathbf{r}_i - \mathbf{r}_j|} \\ & - \frac{1}{4\pi\epsilon_0} \sum_n^M \sum_i^N \frac{Z_n e^2}{|\mathbf{r}_i - \mathbf{R}_n|} + \frac{1}{4\pi\epsilon_0} \frac{1}{2} \sum_{n,m=1; n \neq m}^M \frac{Z_n Z_m e^2}{|\mathbf{R}_n - \mathbf{R}_m|}\end{aligned}$$

with

$$\hat{H} = \hat{T}_e$$

The kinetic energy operators for each electron in the system

The Many Body Hamiltonian

Basic Hamiltonian of a system of N electrons and M nuclei

$$\hat{H} = -\frac{\hbar^2}{2m_e} \sum_{i=1}^N \nabla_i^2 - \sum_{n=1}^M \frac{\hbar^2}{2M_n} \nabla_n^2 + \frac{1}{4\pi\epsilon_0} \frac{1}{2} \sum_{i,j=1; i \neq j}^N \frac{e^2}{|\mathbf{r}_i - \mathbf{r}_j|} - \frac{1}{4\pi\epsilon_0} \sum_n^M \sum_i^N \frac{Z_n e^2}{|\mathbf{r}_i - \mathbf{R}_n|} + \frac{1}{4\pi\epsilon_0} \frac{1}{2} \sum_{n,m=1; n \neq m}^M \frac{Z_n Z_m e^2}{|\mathbf{R}_n - \mathbf{R}_m|}$$

with

$$\hat{H} = \hat{T}_e + \hat{T}_n$$

The kinetic energy operators for each nucleus in the system

The Many Body Hamiltonian

Basic Hamiltonian of a system of N electrons and M nuclei

$$\hat{H} = -\frac{\hbar^2}{2m_e} \sum_{i=1}^N \nabla_i^2 - \sum_{n=1}^M \frac{\hbar^2}{2M_n} \nabla_n^2 + \frac{1}{4\pi\epsilon_0} \frac{1}{2} \sum_{i,j=1; i \neq j}^N \frac{e^2}{|\mathbf{r}_i - \mathbf{r}_j|} - \frac{1}{4\pi\epsilon_0} \sum_n^M \sum_i^N \frac{Z_n e^2}{|\mathbf{r}_i - \mathbf{R}_n|} + \frac{1}{4\pi\epsilon_0} \frac{1}{2} \sum_{n,m=1; n \neq m}^M \frac{Z_n Z_m e^2}{|\mathbf{R}_n - \mathbf{R}_m|}$$

with

$$\hat{H} = \hat{T}_e + \hat{T}_n + \hat{U}_{ee}$$

The potential energy arising from Coulombic electron-electron repulsions

The Many Body Hamiltonian

Basic Hamiltonian of a system of N electrons and M nuclei

$$\hat{H} = -\frac{\hbar^2}{2m_e} \sum_{i=1}^N \nabla_i^2 - \sum_{n=1}^M \frac{\hbar^2}{2M_n} \nabla_n^2 + \frac{1}{4\pi\epsilon_0} \frac{1}{2} \sum_{i,j=1; i \neq j}^N \frac{e^2}{|\mathbf{r}_i - \mathbf{r}_j|}$$
$$-\frac{1}{4\pi\epsilon_0} \sum_n^M \sum_i^N \frac{Z_n e^2}{|\mathbf{r}_i - \mathbf{R}_n|} + \frac{1}{4\pi\epsilon_0} \frac{1}{2} \sum_{n,m=1; n \neq m}^M \frac{Z_n Z_m e^2}{|\mathbf{R}_n - \mathbf{R}_m|}$$

with

$$\hat{H} = \hat{T}_e + \hat{T}_n + \hat{U}_{ee} + \hat{U}_{en}$$

The potential energy between the electrons and nuclei - the total electron-nucleus Coulombic attraction in the system

The Many Body Hamiltonian

Basic Hamiltonian of a system of N electrons and M nuclei

$$\hat{H} = -\frac{\hbar^2}{2m_e} \sum_{i=1}^N \nabla_i^2 - \sum_{n=1}^M \frac{\hbar^2}{2M_n} \nabla_n^2 + \frac{1}{4\pi\epsilon_0} \frac{1}{2} \sum_{i,j=1; i \neq j}^N \frac{e^2}{|\mathbf{r}_i - \mathbf{r}_j|} - \frac{1}{4\pi\epsilon_0} \sum_n^M \sum_i^N \frac{Z_n e^2}{|\mathbf{r}_i - \mathbf{R}_n|} + \frac{1}{4\pi\epsilon_0} \frac{1}{2} \sum_{n,m=1; n \neq m}^M \frac{Z_n Z_m e^2}{|\mathbf{R}_n - \mathbf{R}_m|}$$

with

$$\hat{H} = \hat{T}_e + \hat{T}_n + \hat{U}_{ee} + \hat{U}_{en} + \hat{U}_{nn}$$

The potential energy arising from Coulombic nuclei-nuclei repulsions

One Hamiltonian two communities

First principles (*Ab initio*)

Solution of the many body
Schrödinger equation

$$\hat{H}\Psi = E\Psi$$

- No empirical assumptions
- No fitting parameters*
- Full electronic structure**
- Different level of accuracy
(approximations)
- Atomistic interpretation

One Hamiltonian two communities

First principles (*Ab initio*)

Solution of the many body
Schrödinger equation

$$\hat{H}\Psi = E\Psi$$

- No empirical assumptions
- No fitting parameters*
- Full electronic structure**
- Different level of accuracy (approximations)
- Atomistic interpretation

Model Hamiltonian

Solution of simplified lattice fermion models
(typically the Hubbard model)

$$H = -t \sum_{\langle i,j \rangle, \sigma} (c_{i,\sigma}^\dagger c_{j,\sigma} + c_{j,\sigma}^\dagger c_{i,\sigma}) + U \sum_{i=1}^N n_{i\uparrow} n_{i\downarrow}$$

- Restricted Hilbert space (few bands near E_F)
- Short-ranged electron interactions
- Adjustable parameters
- Accurate solution, transparent physical interpretation

One Hamiltonian two communities

First principles (*Ab initio*)

Solution of the many body
Schrödinger equation

$$\hat{H}\Psi = E\Psi$$

- No empirical assumptions
- No fitting parameters*
- Full electronic structure**
- Different level of accuracy (approximations)
- Atomistic interpretation

Model Hamiltonian

Solution of simplified lattice fermion models
(typically the Hubbard model)

$$H = -t \sum_{\langle i,j \rangle, \sigma} (c_{i,\sigma}^\dagger c_{j,\sigma} + c_{j,\sigma}^\dagger c_{i,\sigma}) + U \sum_{i=1}^N n_{i\uparrow} n_{i\downarrow}$$

- Restricted Hilbert space (few bands near E_F)
- Short-ranged electron interactions
- Adjustable parameters
- Accurate solution, transparent physical interpretation

$$\text{FP+MH} \rightarrow DFT(GW) + DMFT$$

First principles

Approximations

$$\hat{H}\Psi = E\Psi$$

- ① Born-Oppenheimer approximation

$$\hat{H}_e\Psi = E\Psi, \quad \hat{H}_e = T_e + V_{ee} + V_{en}$$

Approximations

$$\hat{H}\Psi = E\Psi$$

- ① Born-Oppenheimer approximation

$$\hat{H}_e\Psi = E\Psi, \quad \hat{H}_e = T_e + V_{ee} + V_{en}$$

Many-body $\Psi(\mathbf{r}_1, \dots, \mathbf{r}_N)$ storage requirements prohibitive

$$(\# \text{grid points})^N$$

- ② Map to "one-electron" theory

Density Functional Theory (LDA, GGA)
&
Hartree-Fock (EXX)

First principles

Approximations

$$\hat{H}\Psi = E\Psi$$

- ① Born-Oppenheimer approximation

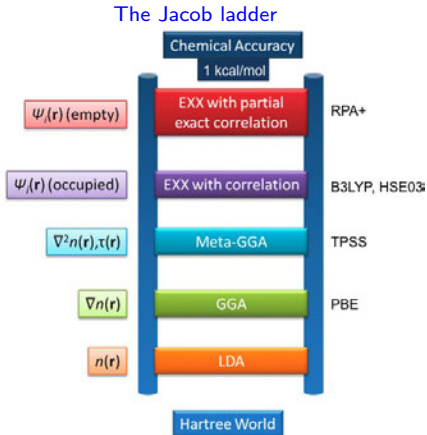
$$\hat{H}_e\Psi = E\Psi, \quad \hat{H}_e = T_e + V_{ee} + V_{en}$$

Many-body $\Psi(\mathbf{r}_1, \dots, \mathbf{r}_N)$ storage requirements prohibitive

$$(\# \text{grid points})^N$$

- ② Map to "one-electron" theory

Density Functional Theory (LDA, GGA)
&
Hartree-Fock (EXX)



Solution of the full electronic Schrödinger equation

$$\hat{H}_e \Psi = E \Psi$$

Hartree: non-interacting (NI) particles (independent particle approximation)

$$\Psi^{HP}(\mathbf{x}_1, \mathbf{x}_2, \dots, \mathbf{x}_N) = \phi_1(\mathbf{x}_1) \phi_2(\mathbf{x}_2) \dots \phi_N(\mathbf{x}_N)$$

where $\phi(\mathbf{x})$ is an eigenstate of:

$$\hat{H}_e^{NI} = -\frac{\hbar^2}{2m_e} \sum_{i=1}^N \nabla_i^2 - \frac{1}{4\pi\epsilon_0} \sum_n^M \sum_i^N \frac{Z_n e^2}{|\mathbf{r}_i - \mathbf{R}_n|} = \sum_{i=1}^N h(\mathbf{r}_i)$$

Variational principle:

$$\langle H_e \rangle \equiv \frac{\langle \Psi^{HP} | \hat{H}_e | \Psi^{HP} \rangle}{\langle \Psi^{HP} | \Psi^{HP} \rangle} \geq E_0$$

The Hartree World:

$$\Psi^{HP}(\mathbf{x}_1, \mathbf{x}_2, \dots, \mathbf{x}_N) = \phi_1(\mathbf{x}_1) \phi_2(\mathbf{x}_2) \dots \phi_N(\mathbf{x}_N)$$

Limitation of the Hartree product:

- ① *Uncorrelated probability distribution:*

$$\rho(\mathbf{x}_1, \mathbf{x}_2, \dots, \mathbf{x}_N) = |\phi_1(\mathbf{x}_1)|^2 |\phi_2(\mathbf{x}_2)|^2 \dots |\phi_N(\mathbf{x}_N)|^2$$

The interaction among particles taken into account through the [Hartree term](#), i.e. electrostatic potential arising from the charge distribution of N electrons:

$$\sum_{i=1}^N \int d\mathbf{x}' |\phi_i(\mathbf{x}')|^2 \frac{1}{|\mathbf{r} - \mathbf{r}'|}$$

The Hartree World:

$$\Psi^{HP}(\mathbf{x}_1, \mathbf{x}_2, \dots, \mathbf{x}_N) = \phi_1(\mathbf{x}_1) \phi_2(\mathbf{x}_2) \dots \phi_N(\mathbf{x}_N)$$

Limitation of the Hartree product:

- ① *Uncorrelated probability distribution:*

$$\rho(\mathbf{x}_1, \mathbf{x}_2, \dots, \mathbf{x}_N) = |\phi_1(\mathbf{x}_1)|^2 |\phi_2(\mathbf{x}_2)|^2 \dots |\phi_N(\mathbf{x}_N)|^2$$

The interaction among particles taken into account through the [Hartree term](#), i.e. electrostatic potential arising from the charge distribution of N electrons:

$$\sum_{i=1}^N \int d\mathbf{x}' |\phi_i(\mathbf{x}')|^2 \frac{1}{|\mathbf{r} - \mathbf{r}'|}$$

- ② *Self interaction error:*

The Hartree-term includes a sum over all electrons

The Hartree World:

$$\Psi^{HP}(\mathbf{x}_1, \mathbf{x}_2, \dots, \mathbf{x}_N) = \phi_1(\mathbf{x}_1) \phi_2(\mathbf{x}_2) \dots \phi_N(\mathbf{x}_N)$$

Limitation of the Hartree product:

- ① *Uncorrelated probability distribution:*

$$\rho(\mathbf{x}_1, \mathbf{x}_2, \dots, \mathbf{x}_N) = |\phi_1(\mathbf{x}_1)|^2 |\phi_2(\mathbf{x}_2)|^2 \dots |\phi_N(\mathbf{x}_N)|^2$$

The interaction among particles taken into account through the [Hartree term](#), i.e. electrostatic potential arising from the charge distribution of N electrons:

$$\sum_{i=1}^N \int d\mathbf{x}' |\phi_i(\mathbf{x}')|^2 \frac{1}{|\mathbf{r} - \mathbf{r}'|}$$

- ② *Self interaction error:*

The Hartree-term includes a sum over all electrons

- ③ Ψ^{HP} is *not Antisymmetric*

$$\mathcal{P}_{1,2} [\psi_1(\mathbf{x}_1) \psi_2(\mathbf{x}_2) \dots \psi_N(\mathbf{x}_N)] = \psi_1(\mathbf{x}_2) \psi_2(\mathbf{x}_1) \dots \psi_N(\mathbf{x}_N) \neq -\psi_1(\mathbf{x}_1) \psi_2(\mathbf{x}_2) \dots \psi_N(\mathbf{x}_N)$$

The Hartree-Fock Theory

In the HF method the WF the WF is written as a Slater determinant.

$$\Psi^{HP}(\mathbf{x}_1, \mathbf{x}_2, \dots, \mathbf{x}_N) = \phi_1(\mathbf{x}_1) \phi_2(\mathbf{x}_2) \dots \phi_N(\mathbf{x}_N)$$

\Downarrow

$$\Psi_{AS}(\mathbf{x}_1, \mathbf{x}_2, \dots, \mathbf{x}_N) = \frac{1}{\sqrt{N!}} \begin{vmatrix} \phi_1(\mathbf{x}_1) & \phi_2(\mathbf{x}_1) & \dots & \phi_N(\mathbf{x}_1) \\ \phi_1(\mathbf{x}_2) & \phi_2(\mathbf{x}_2) & \dots & \phi_N(\mathbf{x}_2) \\ \vdots & \vdots & & \vdots \\ \phi_1(\mathbf{x}_N) & \phi_2(\mathbf{x}_N) & \dots & \phi_N(\mathbf{x}_N) \end{vmatrix}$$

The Hartree-Fock Theory

In the HF method the WF the WF is written as a Slater determinant.

$$\Psi^{HP}(\mathbf{x}_1, \mathbf{x}_2, \dots, \mathbf{x}_N) = \phi_1(\mathbf{x}_1) \phi_2(\mathbf{x}_2) \dots \phi_N(\mathbf{x}_N)$$
$$\Downarrow$$
$$\Psi_{AS}(\mathbf{x}_1, \mathbf{x}_2, \dots, \mathbf{x}_N) = \frac{1}{\sqrt{N!}} \begin{vmatrix} \phi_1(\mathbf{x}_1) & \phi_2(\mathbf{x}_1) & \dots & \phi_N(\mathbf{x}_1) \\ \phi_1(\mathbf{x}_2) & \phi_2(\mathbf{x}_2) & \dots & \phi_N(\mathbf{x}_2) \\ \vdots & \vdots & & \vdots \\ \phi_1(\mathbf{x}_N) & \phi_2(\mathbf{x}_N) & \dots & \phi_N(\mathbf{x}_N) \end{vmatrix}$$

- ① **Antisymmetric**
- ② **Self interaction free**
- ③ **Uncorrelated**

Only particles with the same spin have a certain degree of correlation:

$$\rho(\mathbf{x}_1, \mathbf{x}_2) = 0 \text{ if } \mathbf{r}_1 = \mathbf{r}_2$$

Pauli principle

The Hartree-Fock Theory

The Hartree-Fock equations:

- ① Electronic Hamiltonian $\hat{H}_e = T_e + V_{ee} + V_{en}$

$$\hat{H}_e = -\frac{1}{2} \sum_{i=1}^N \nabla_i^2 + \frac{1}{2} \sum_{i,j=1; i \neq j}^N \frac{e^2}{|\mathbf{r}_i - \mathbf{r}_j|} - \sum_n^M \sum_i^N \frac{Z_n e^2}{|\mathbf{r}_i - \mathbf{R}_n|}$$

- ② WF \rightarrow Slater determinant Ψ_{AS}

③ $\langle \Psi_{AS} | \hat{H}_e | \Psi_{AS} \rangle$

- ④ Variation principle

↓

$$\begin{aligned} & \left[-\frac{1}{2} \nabla^2 - \sum_n \frac{Z_n}{|\mathbf{r} - \mathbf{R}_n|} \right] \psi_k(\mathbf{x}) + \sum_{l=1}^N \int d\mathbf{x}' |\psi_l(\mathbf{x}')|^2 \frac{1}{|\mathbf{r} - \mathbf{r}'|} \psi_k(\mathbf{x}) \\ & - \sum_{l=1}^N \int d\mathbf{x}' \psi_l^*(\mathbf{x}') \frac{1}{|\mathbf{r} - \mathbf{r}'|} \psi_k(\mathbf{x}') \psi_l(\mathbf{x}) = \epsilon_k \psi_k \end{aligned}$$

It has the form of a Schrödinger equation, where the eigenvalues ϵ_k represent the orbital energies. One more term: EXCHANGE.

The Hartree-Fock Theory

$$\hat{\mathcal{F}}\psi_k = \left[-\frac{1}{2}\nabla^2 - \sum_n \frac{Z_n}{|\mathbf{r} - \mathbf{R}_n|} \right] \psi_k(\mathbf{x}) + \sum_{l=1}^N \int d\mathbf{x}' |\psi_l(\mathbf{x}')|^2 \frac{1}{|\mathbf{r} - \mathbf{r}'|} \psi_k(\mathbf{x})$$
$$- \sum_{l=1}^N \int d\mathbf{x}' \psi_l^*(\mathbf{x}') \frac{1}{|\mathbf{r} - \mathbf{r}'|} \psi_k(\mathbf{x}') \psi_l(\mathbf{x}) = \epsilon_k \psi_k$$

- ① Hartree term only: unphysical coupling between orbital k and itself (self-energy)
- ② Exchange term non-local: its value at \mathbf{r} depends on $\psi_k(\mathbf{r}')$

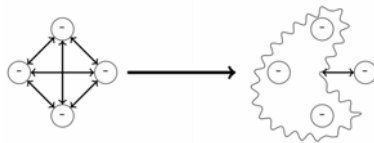
The Exchange term is the same as the Hartree term, with two spin-orbitals labels k and l interchanged and a *minus sign*.

- ③ Fock+Hartree: self-energy problem solved

The Fock operator $\hat{\mathcal{F}}$ is a one particle operator. It replaces the many-body Schrödinger equation by a set of one-particle equations, in which each electron moves in an effective field, often also called *mean-field*.

The Hartree-Fock Theory

The Fock operator $\hat{\mathcal{F}}$ is a one particle operator. It replaces the many-body Schrödinger equation by a set of one-particle equations, in which each electron moves in an effective **mean-field**.



Many-body problem → one-electron problems

The WF does not have explicit dependence on the position of all other electrons. The dependence is only implicit via the Exchange term.

Density Functional Theory

Hartree-Fock equations:

$$\left(-\frac{\hbar^2}{2m_e} \nabla^2 + V_e(\mathbf{r}) + V_H(\mathbf{r}) \right) \phi_i(\mathbf{r}) + \int V_x(\mathbf{r}, \mathbf{r}') \phi_i(\mathbf{r}') d^3 r' = \epsilon_i^{HF} \phi_i(\mathbf{r})$$

- Mean-field
- WF-based method: Slater determinant
- exact exchange V_x
- no correlation (only Pauli principle)
- Self-interaction free

Density Functional Theory

Hartree-Fock equations:

$$\left(-\frac{\hbar^2}{2m_e} \nabla^2 + V_e(\mathbf{r}) + V_H(\mathbf{r}) \right) \phi_i(\mathbf{r}) + \int V_x(\mathbf{r}, \mathbf{r}') \phi_i(\mathbf{r}') d^3 r' = \epsilon_i^{HF} \phi_i(\mathbf{r})$$

- Mean-field
- WF-based method: Slater determinant
- exact exchange V_x
- no correlation (only Pauli principle)
- Self-interaction free

DFT equations:

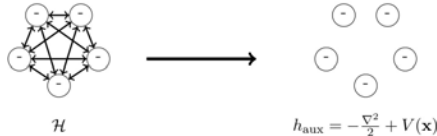
$$\left(-\frac{\hbar^2}{2m_e} \nabla^2 + V_{en}(\mathbf{r}) + V_H + V_{xc}(\mathbf{r}) \right) \phi_i(\mathbf{r}) = \epsilon_i^{KS} \phi_i(\mathbf{r})$$

- ① Mean-field
- ② Density-based method
- ③ approximate exchange & correlation, V_{xc}
- ④ Self-interaction problem

Density Functional Theory

① Mean-field

The real interacting system is replaced by an effective Kohn-Sham (KS) system of non-interacting electrons in an effective potential V .



$$H \rightarrow \sum_{i=1}^N h_{aux}; \quad h_{aux}\phi_i = \epsilon_i\phi_i; \quad \phi_i = \text{KS single-particle orbitals}$$

② Density-based method

The DFT approach promotes the particle density

$$n(\mathbf{r}) = \sum_{i, \text{occupied}} |\phi_i(\mathbf{r})|^2.$$

to the status of key variable, on which the calculation of all other observables can be based (Hohenberg-Kohn Theorem)

$$\begin{array}{ccc} V_{ext}(\mathbf{r}) & \xleftarrow{HK} & n_0(\mathbf{r}) \\ \downarrow & & \uparrow \\ \Psi_i(\mathbf{r}) & \Rightarrow & \Psi_0(\mathbf{r}) \end{array}$$

Density Functional Theory

- ③ approximate exchange and correlation, V_{xc}

Universal functional for the energy given in terms of the density:

$$E[n] = T_{KS}[n] + \int d^3n(\mathbf{r})V_{ext}(\mathbf{r}) + \frac{e^2}{2} \int \int d^3rd^3r' \frac{n(\mathbf{r})n(\mathbf{r}')}{|\mathbf{r} - \mathbf{r}'|} + E_{xc}[n]$$

$$E[n] \geq E[n_{GS}] = E_{GS}^{True}$$

The quality of the solution depend on the (*unknown*) form of the XC potential V_{xc} :

$$V_{xc}([n], \mathbf{r}) = \frac{\delta E_{XC}}{\delta n(\mathbf{r})}$$

Approximations needed:

$$E_{xc}^{LDA}[n] = \int dr^3 e_{xc}(n(\mathbf{r}))$$

$$E_{xc}^{GGA}[n] = \int dr^3 f(n(\mathbf{r}), \nabla n(\mathbf{r}))$$

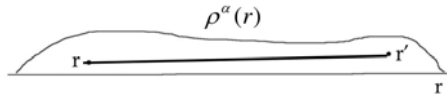
Density Functional Theory

④ Self-interaction problem

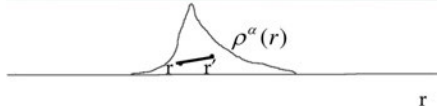
Non complete cancellation of the spurious repulsion of each electron from itself, included in the Hartree term, that is not completely accounted for in XC functionals:

$$\Delta\epsilon = \int \int \frac{n_1(\mathbf{r})n_1(\mathbf{r}')}{|\mathbf{r} - \mathbf{r}'|} d\mathbf{r} d\mathbf{r}'$$

Delocalized States → small Errors



Localized States → large Errors



Hands-on: DFT & HF (VASP)

Hartree-Fock equations:

$$\left(-\frac{\hbar^2}{2m_e} \nabla^2 + V_e(\mathbf{r}) + V_H(\mathbf{r}) \right) \phi_i(\mathbf{r}) + \int V_x(\mathbf{r}, \mathbf{r}') \phi_i(\mathbf{r}') d^3 r' = \epsilon_i^{HF} \phi_i(\mathbf{r})$$

- Mean-field
- WF-based method: Slater determinant
- exact exchange V_x
- no correlation (only Pauli principle)
- Self-interaction free

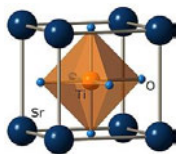
DFT equations:

$$\left(-\frac{\hbar^2}{2m_e} \nabla^2 + V_{en}(\mathbf{r}) + V_H + V_{xc}(\mathbf{r}) \right) \phi_i(\mathbf{r}) = \epsilon_i^{KS} \phi_i(\mathbf{r})$$

- ① Mean-field
- ② Density-based method
- ③ approximate exchange & correlation, V_{xc}
- ④ Self-interaction problem

Hands-on: DFT & HF (VASP)

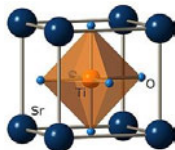
Test case: SrTiO₃



	DFT(GGA)	HF	Expt.
Direct gap (eV) $\Gamma - \Gamma$?	?	3.75
Running time	?	?	

Hands-on: DFT & HF (VASP)

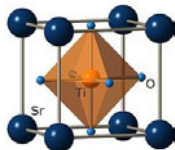
Test case: SrTiO₃



	DFT(GGA)	HF	Expt.
Direct gap (eV) $(\Gamma - \Gamma)$	2.16	4.66	3.75
CPU time (s)	5	613	

Hands-on: DFT & HF (VASP)

Test case: SrTiO₃



	DFT(GGA)	HF	Expt.
Direct gap (eV) $(\Gamma - \Gamma)$	2.16	4.66	3.75
CPU time (s)	5	613	

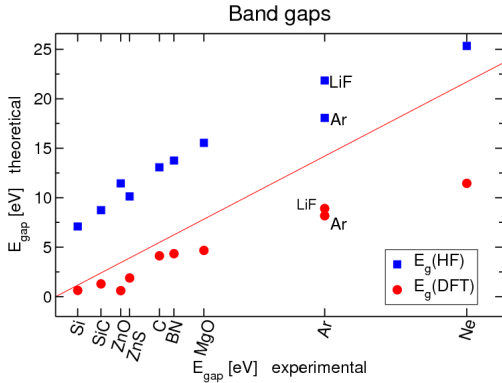
DFT

- ① band gap too small
(self-interaction problem)
- ② fast
(approx. E_{xc})

HF

- ① band gap too large
(no correlation)
- ② slow
(two-particle integral, exact exchange)

DFT vs. HF

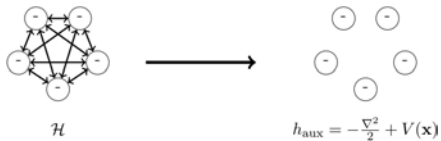


General trend: DFT tends to underestimate band gaps, HF overestimates

DFT + HF ?

Hybrid Functionals

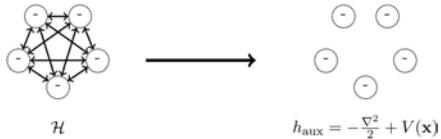
Adiabatic connection and coupling-constant integration



The adiabatic connection continuously transform the real interacting system to the non-interacting one

Hybrid Functionals

Adiabatic connection and coupling-constant integration



The adiabatic connection continuously transform the real interacting system to the non-interacting one

$$V_{ee} \rightarrow \lambda V_{ee} \quad \text{with} \quad 0 \leq \lambda \leq 1$$

$\lambda = 0$: non-interacting KS system $\rightarrow \Psi_{\lambda=0}$ = KS-WF

$\lambda = 1$: exact many-body systems $\rightarrow \Psi_{\lambda=1}$ = Exact many-body WF

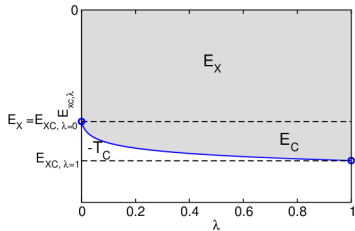
$$E_{XC} = \int_0^1 E_{xc,\lambda} d\lambda, \quad E_{xc,\lambda} = \langle \Psi_\lambda | V_{ee} | \Psi_\lambda \rangle - E_H$$

Hybrid Functionals

Adiabatic connection and coupling-constant integration

$$E_{XC} = \int_0^1 E_{xc,\lambda} d\lambda, \quad E_{xc,\lambda} = \langle \Psi_\lambda | V_{ee} | \Psi_\lambda \rangle - E_H$$

$E_{xc,\lambda}$ is a monotonically decreasing function of λ



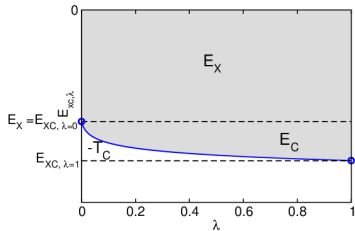
The area between the curve and the x-axis is just E_{xc} .

Hybrid Functionals

Adiabatic connection and coupling-constant integration

$$E_{XC} = \int_0^1 E_{xc,\lambda} d\lambda, \quad E_{xc,\lambda} = \langle \Psi_\lambda | V_{ee} | \Psi_\lambda \rangle - E_H$$

$E_{xc,\lambda}$ is a monotonically decreasing function of λ



The area between the curve and the x-axis is just E_{xc} .

The integral can be approximated via linear interpolation:

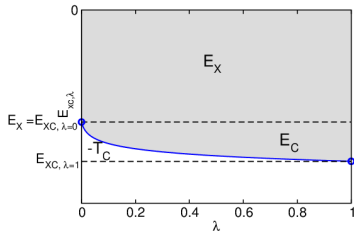
$$E_{XC} \approx \frac{1}{2} E_{XC,\lambda=0} + \frac{1}{2} E_{XC,\lambda=1}$$

Hybrid Functionals

Adiabatic connection and coupling-constant integration

$$E_{XC} = \int_0^1 E_{xc,\lambda} d\lambda, \quad E_{xc,\lambda} = \langle \Psi_\lambda | V_{ee} | \Psi_\lambda \rangle - E_H$$

$E_{xc,\lambda}$ is a monotonically decreasing function of λ



The area between the curve and the x-axis is just E_{xc} .

The integral can be approximated via linear interpolation:

$$E_{XC} \approx \frac{1}{2} E_{XC,\lambda=0} + \frac{1}{2} E_{XC,\lambda=1} \Rightarrow \boxed{E_{XC}^{\text{Hybrid}} = \frac{1}{2} E_X^{\text{HF}} + \frac{1}{2} E_{XC}^{\text{LDA}}}$$

The Hybrid Functionals Family

Half-Half, Becke 1993

$$E_{XC}^{\text{Hybrid}} = \frac{1}{2} E_X^{HF} + \frac{1}{2} E_{XC}^{LDA}$$

The Hybrid Functionals Family

Half-Half, Becke 1993

$$E_{XC}^{\text{Hybrid}} = \frac{1}{2} E_X^{HF} + \frac{1}{2} E_{XC}^{LDA}$$

B3LYP, Becke 1993-1994

$$E_{XC}^{\text{B3LYP}} = E_X^{LDA} + \alpha_1(E_X^{HF} - E_X^{LDA}) + \alpha_2(E_X^{GGA} - E_X^{LDA}) + \alpha_3(E_C^{GGA} - E_C^{LDA})$$

The Hybrid Functionals Family

Half-Half, Becke 1993

$$E_{XC}^{\text{Hybrid}} = \frac{1}{2} E_X^{HF} + \frac{1}{2} E_{XC}^{LDA}$$

B3LYP, Becke 1993-1994

$$E_{XC}^{\text{B3LYP}} = E_X^{LDA} + \alpha_1(E_X^{HF} - E_X^{LDA}) + \alpha_2(E_X^{GGA} - E_X^{LDA}) + \alpha_3(E_C^{GGA} - E_C^{LDA})$$

PBE0, Perdew-Burke-Ernzerhof 1996

$$E_{XC}^{\text{PBE0}} = E_C^{PBE} + \alpha E_X^{HF} + (1 - \alpha) E_X^{PBE},$$

The Hybrid Functionals Family

Half-Half, Becke 1993

$$E_{XC}^{\text{Hybrid}} = \frac{1}{2} E_X^{HF} + \frac{1}{2} E_X^{LDA}$$

B3LYP, Becke 1993-1994

$$E_{XC}^{\text{B3LYP}} = E_X^{LDA} + \alpha_1(E_X^{HF} - E_X^{LDA}) + \alpha_2(E_X^{GGA} - E_X^{LDA}) + \alpha_3(E_C^{GGA} - E_C^{LDA})$$

PBE0, Perdew-Burke-Ernzerhof 1996

$$E_{XC}^{\text{PBE0}} = E_C^{PBE} + \alpha E_X^{HF} + (1 - \alpha) E_X^{PBE},$$

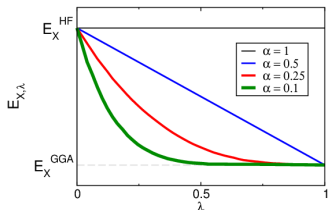
Choice of α

Optimum: $\alpha = 0.25$ (fit to MP2) →

In practice α is system dependent

Disadvantages

Long-range E_X numerically complicated



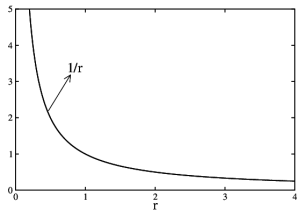
Screened Hybrid Functionals: HSE

From PBE0 to HSE

$$V_x \rightarrow V_{sx}$$

$$-e^2 \frac{\sum_j f_j \phi_j(\mathbf{r}) \phi_j^*(\mathbf{r}')}{|\mathbf{r} - \mathbf{r}'|} \rightarrow -e^2 \sum_j f_j \phi_j(\mathbf{r}) \phi_j^*(\mathbf{r}') \frac{\text{erfc}(\mu |\mathbf{r} - \mathbf{r}'|)}{|\mathbf{r} - \mathbf{r}'|}$$

$$\frac{1}{r} = \frac{\text{erfc}(\mu r)}{sr} + \frac{\text{erf}(\mu r)}{lr}$$



$$E_{XC}^{\text{HSE}} = \alpha E_X^{\text{HF}, sr}(\mu) + (1 - \alpha) E_X^{\text{PBE}, sr}(\mu) + \alpha E_X^{\text{PBE}, lr}(\mu) + E_C^{\text{PBE}}$$

Default values:

$$\alpha = 0.25;$$

$$\mu = 0.2 \text{ \AA}^{-1}$$

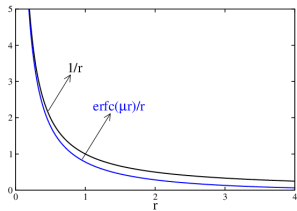
Screened Hybrid Functionals: HSE

From PBE0 to HSE

$$V_x \rightarrow V_{sx}$$

$$-e^2 \frac{\sum_j f_j \phi_j(\mathbf{r}) \phi_j^*(\mathbf{r}')}{|\mathbf{r} - \mathbf{r}'|} \rightarrow -e^2 \sum_j f_j \phi_j(\mathbf{r}) \phi_j^*(\mathbf{r}') \frac{\text{erfc}(\mu |\mathbf{r} - \mathbf{r}'|)}{|\mathbf{r} - \mathbf{r}'|}$$

$$\frac{1}{r} = \frac{\text{erfc}(\mu r)}{sr} + \frac{\text{erf}(\mu r)}{lr}$$



$$E_{XC}^{\text{HSE}} = \alpha E_X^{\text{HF}, sr}(\mu) + (1 - \alpha) E_X^{\text{PBE}, sr}(\mu) + \alpha E_X^{\text{PBE}, lr}(\mu) + E_C^{\text{PBE}}$$

Default values:

$$\alpha = 0.25;$$

$$\mu = 0.2 \text{ \AA}^{-1}$$

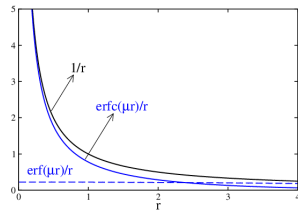
Screened Hybrid Functionals: HSE

From PBE0 to HSE

$$V_x \rightarrow V_{sx}$$

$$-e^2 \frac{\sum_j f_j \phi_j(\mathbf{r}) \phi_j^*(\mathbf{r}')}{|\mathbf{r} - \mathbf{r}'|} \rightarrow -e^2 \sum_j f_j \phi_j(\mathbf{r}) \phi_j^*(\mathbf{r}') \frac{\operatorname{erfc}(\mu |\mathbf{r} - \mathbf{r}'|)}{|\mathbf{r} - \mathbf{r}'|}$$

$$\frac{1}{r} = \frac{\operatorname{erfc}(\mu r)}{sr} + \frac{\operatorname{erf}(\mu r)}{lr}$$



$$E_{XC}^{\text{HSE}} = \alpha E_X^{\text{HF}, sr}(\mu) + (1 - \alpha) E_X^{\text{PBE}, sr}(\mu) + \alpha E_X^{\text{PBE}, lr}(\mu) + E_C^{\text{PBE}}$$

Default values:

$$\alpha = 0.25;$$

$$\mu = 0.2 \text{ \AA}^{-1}$$

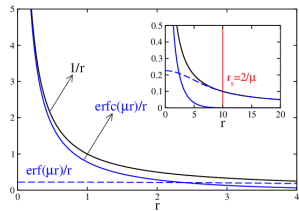
Screened Hybrid Functionals: HSE

From PBE0 to HSE

$$V_x \rightarrow V_{sx}$$

$$-e^2 \frac{\sum_j f_j \phi_j(\mathbf{r}) \phi_j^*(\mathbf{r}')}{|\mathbf{r} - \mathbf{r}'|} \rightarrow -e^2 \sum_j f_j \phi_j(\mathbf{r}) \phi_j^*(\mathbf{r}') \frac{\operatorname{erfc}(\mu |\mathbf{r} - \mathbf{r}'|)}{|\mathbf{r} - \mathbf{r}'|}$$

$$\frac{1}{r} = \frac{\operatorname{erfc}(\mu r)}{sr} + \frac{\operatorname{erf}(\mu r)}{lr}$$



$$E_{XC}^{\text{HSE}} = \alpha E_X^{HF,sr}(\mu) + (1 - \alpha) E_X^{PBE,sr}(\mu) + \alpha E_X^{PBE,lr}(\mu) + E_C^{PBE}$$

Default values:

$$\alpha = 0.25;$$

$$\mu = 0.2 \text{ \AA}^{-1}$$

Screened Hybrid Functionals

Why Screening

- Computational convenience: neglect numerically complex long-range part of E_X
- Physical justification: in many-body systems the unscreened exchange is reduced

Screened Hybrid Functionals

Why Screening

- Computational convenience: neglect numerically complex long-range part of E_X
- Physical justification: in many-body systems the unscreened exchange is reduced

Hybrid Functionals meets GW

- DFT

$$\left(-\frac{1}{2}\Delta + V_{\text{ext}}(\mathbf{r}) + V_{\text{H}}(\mathbf{r}) + V_{\text{xc}}(\mathbf{r}) \right) \psi_{n\mathbf{k}}(\mathbf{r}) = \epsilon_{n\mathbf{k}} \psi_{n\mathbf{k}}(\mathbf{r})$$

- HF

$$\left(-\frac{1}{2}\Delta + V_{\text{ext}}(\mathbf{r}) + V_{\text{H}}(\mathbf{r}) \right) \psi_{n\mathbf{k}}(\mathbf{r}) + \int V_{\text{X}}(\mathbf{r}, \mathbf{r}') \psi_{n\mathbf{k}}(\mathbf{r}') d\mathbf{r}' = \epsilon_{n\mathbf{k}} \psi_{n\mathbf{k}}(\mathbf{r})$$

- HSE

$$\left(-\frac{1}{2}\Delta + V_{\text{ext}}(\mathbf{r}) + V_{\text{H}}(\mathbf{r}) + V_{\text{c}}(\mathbf{r}) \right) \psi_{n\mathbf{k}}(\mathbf{r}) + \int V_{\text{sX}}^{\text{HSE}}(\mathbf{r}, \mathbf{r}') \psi_{n\mathbf{k}}(\mathbf{r}') d\mathbf{r}' = \epsilon_{n\mathbf{k}} \psi_{n\mathbf{k}}(\mathbf{r})$$

- Quasiparticle equations (GW)

$$\left(-\frac{1}{2}\Delta + V_{\text{ext}}(\mathbf{r}) + V_{\text{H}}(\mathbf{r}) \right) \psi_{n\mathbf{k}}(\mathbf{r}) + \int \Sigma(\mathbf{r}, \mathbf{r}', E_{n\mathbf{k}}) \psi_{n\mathbf{k}}(\mathbf{r}') d\mathbf{r}' = \epsilon_{n\mathbf{k}} \psi_{n\mathbf{k}}(\mathbf{r})$$

Screened Hybrid Functionals

Hybrid Functionals meets GW

- HSE

$$\left(-\frac{1}{2}\Delta + V_{\text{ext}}(\mathbf{r}) + V_{\text{H}}(\mathbf{r}) + V_{\text{c}}(\mathbf{r}) + \alpha V_{\text{x}}^{lr}(\mathbf{r}) + (1-\alpha)V_{\text{x}}^{sr}(\mathbf{r}) \right) \psi_{n\mathbf{k}}(\mathbf{r}) + \int \alpha V_{\text{x}}^{sr}(\mathbf{r}, \mathbf{r}') \psi_{n\mathbf{k}}(\mathbf{r}') d\mathbf{r}'$$

- Quasiparticle equations (GW)

$$\left(-\frac{1}{2}\Delta + V_{\text{ext}}(\mathbf{r}) + V_{\text{H}}(\mathbf{r}) \right) \psi_{n\mathbf{k}}(\mathbf{r}) + \int \Sigma(\mathbf{r}, \mathbf{r}', E_{n\mathbf{k}}) \psi_{n\mathbf{k}}(\mathbf{r}') d\mathbf{r}'$$

$$\Sigma(\omega) = iG(\omega)W(\omega)$$

W = screened (GW) Coulomb interaction

$$W(\omega) = \epsilon(\omega)^{-1} v \xrightarrow{\epsilon(\omega) \rightarrow \epsilon_\infty = 1/\alpha} \alpha v \xrightarrow{v \rightarrow v_{sr}} \alpha \frac{\operatorname{erfc}(\mu|\mathbf{r} - \mathbf{r}'|)}{|\mathbf{r} - \mathbf{r}'|}$$

Screened Hybrid Functionals

Hybrid Functionals meets GW

- HSE

$$\left(-\frac{1}{2}\Delta + V_{\text{ext}}(\mathbf{r}) + V_{\text{H}}(\mathbf{r}) + V_{\text{c}}(\mathbf{r}) + \alpha V_{\text{x}}^{lr}(\mathbf{r}) + (1-\alpha)V_{\text{x}}^{sr}(\mathbf{r}) \right) \psi_{n\mathbf{k}}(\mathbf{r}) + \int \alpha V_{\text{x}}^{sr}(\mathbf{r}, \mathbf{r}') \psi_{n\mathbf{k}}(\mathbf{r}') d\mathbf{r}'$$

- Quasiparticle equations (GW)

$$\left(-\frac{1}{2}\Delta + V_{\text{ext}}(\mathbf{r}) + V_{\text{H}}(\mathbf{r}) \right) \psi_{n\mathbf{k}}(\mathbf{r}) + \int \Sigma(\mathbf{r}, \mathbf{r}', E_{n\mathbf{k}}) \psi_{n\mathbf{k}}(\mathbf{r}') d\mathbf{r}'$$

$$\Sigma(\omega) = iG(\omega)W(\omega)$$

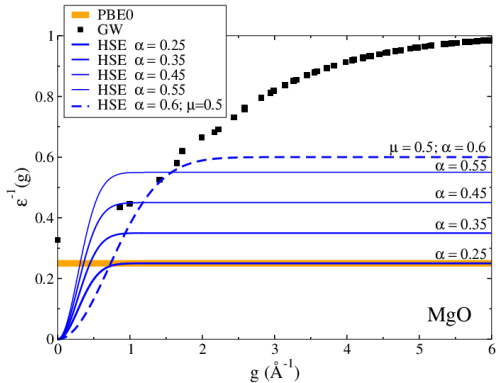
W = screened (GW) Coulomb interaction

$$W(\omega) = \epsilon(\omega)^{-1} v \xrightarrow{\epsilon(\omega) \rightarrow \epsilon_\infty = 1/\alpha} \alpha v \xrightarrow{v \rightarrow v_{sr}} \alpha \frac{\operatorname{erfc}(\mu|\mathbf{r} - \mathbf{r}'|)}{|\mathbf{r} - \mathbf{r}'|}$$

Optimum $\alpha = \frac{1}{\epsilon_\infty}$

Hybrid Functionals

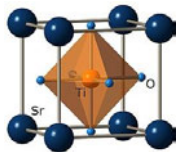
but HSE is NOT GW!



- No Exchange at short wave vector (good only for metals)
- 0.25 choice questionable for wide band gap (small ϵ_∞) materials
better choice $\alpha = \frac{1}{\epsilon_\infty}$
- α and μ fitting parameters

Hands-on: HSE (VASP)

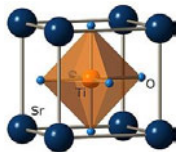
Test case: SrTiO₃



	DFT(GGA)	HF	HSE	Expt.
Direct gap (eV) $(\Gamma - \Gamma')$	2.16	4.66	?	3.75
CPU time (s)	5	613	?	

Hands-on: HSE (VASP)

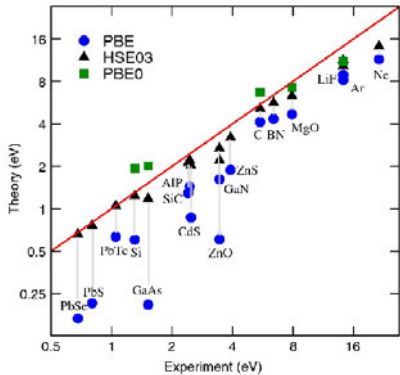
Test case: SrTiO₃



	DFT(GGA)	HF	HSE	Expt.
Direct gap (eV) $(\Gamma - \Gamma')$	2.16	4.66	3.8	3.75
CPU time (s)	5	613	324	

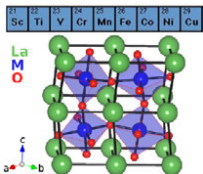
DFT vs. PBE0/HSE

Semiconductors dataset ($\alpha = 0.25$)

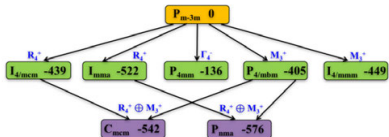
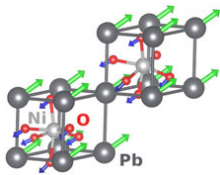
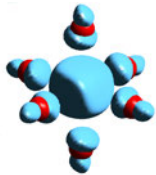
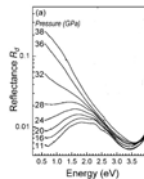


Results

Screened Hybrid Functionals applied to Perovskites

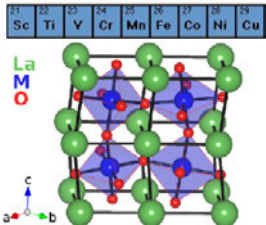


25	26	27
Mn Marguerite 54.938049	Fe Iron 55.845	Co Cobalt 58.933200
43 Tc Tetragonal (98)	44 Ru Ruthenium 101.07	45 Rh Rhodium 102.90550
75 Re Rhodium 186.207	76 Os Osmium 190.23	77 Ir Iridium 192.217



Results: the 3d LaMO_3 perovskite dataset

- Band, Mott-Hubbard, charge-transfer insulator
- NM, A/C/G-AFM, PM
- Orthorhombic, Monoclinic, Rhombohedral, Tetragonal
- t_{2g} , e_g : different degree of (de)localization



LaScO_3	LaTiO_3	LaVO_3	LaCrO_3	LaMnO_3	LaFeO_3	LaCoO_3	LaNiO_3	LaCuO_3
O	O	M	O	O	O	R	R	T
d^0	\uparrow	$\uparrow\uparrow$	$\uparrow\uparrow\uparrow$	$\uparrow\uparrow\uparrow\uparrow$	$\uparrow\uparrow\uparrow\uparrow\uparrow$	$\uparrow\downarrow\downarrow\downarrow\downarrow$	$\uparrow\downarrow\downarrow\downarrow\downarrow\uparrow$	$\uparrow\downarrow\downarrow\downarrow\downarrow\downarrow\uparrow$
							M	M
NM	G-AFM	C-AFM	G-AFM	A-AFM	G-AFM	PM	PM	PM

LDA+U: I. Solovyev, N. Hamada, and K. Terakura, Phys. Rev. B **53**, 7158 (1996).

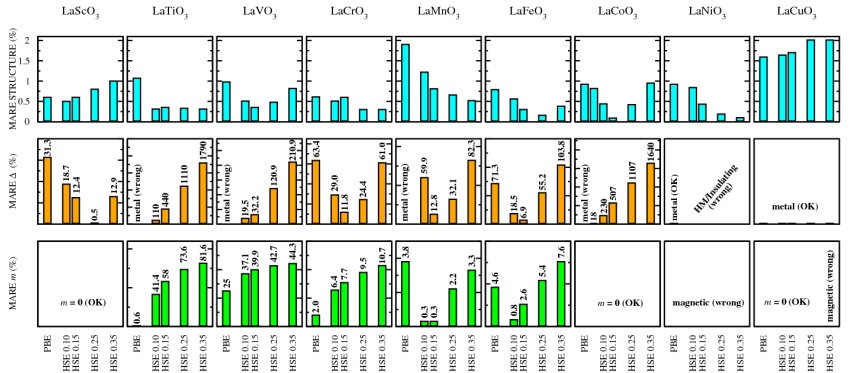
HF: T. Mizokawa and A. Fujimori, Phys. Rev. **54**, 5368 (1996).

GW: Y. Nohara, S. Yamamoto, and T. Fujiwara, Phys. Rev. B **79**, 195110 (2009).

HSE: J. He & C. Franchini, Phys. Rev. B **86**, 235117 (2012).

Results: the 3d LaMO₃ perovskite dataset

Mean absolute relative value (MARE) based on a fitting of **structural properties** (volume, lattice parameters, JT/GFO, ion positions), **band gap**, **magnetic moment**, **spin ordering**.



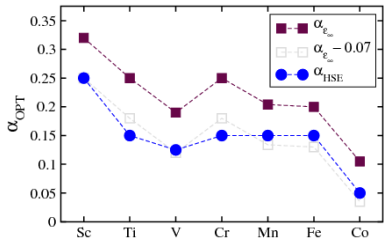
Fitting α

α	LaScO ₃	LaTiO ₃	LaVO ₃	LaCrO ₃	LaMnO ₃	LaFeO ₃	LaCoO ₃	LaNiO ₃	LaCuO ₃
	0.25	0.10 (0.15)	0.10-0.15	0.15	0.15	0.15	0.05	0.0	0.0

Results: the 3d LaMO₃ perovskite dataset

Fitting vs $\alpha_{opt} = 1/\epsilon_\infty$

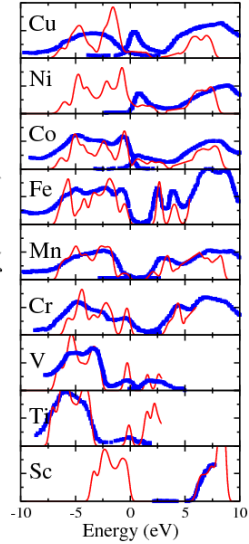
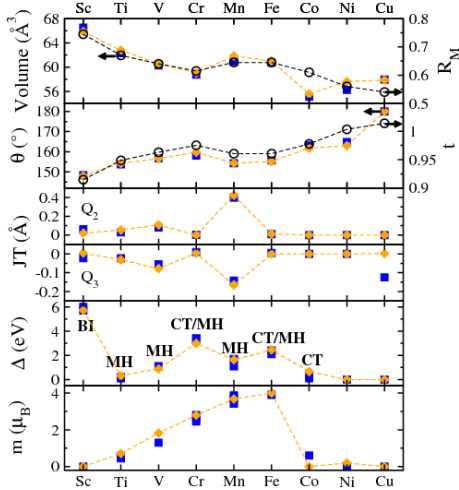
- ① $\alpha_{opt}^{\text{HSE}} \rightarrow \text{HSE fitting}$
- ② $\alpha_{opt}^{\epsilon_\infty} = \frac{1}{\epsilon_\infty}$



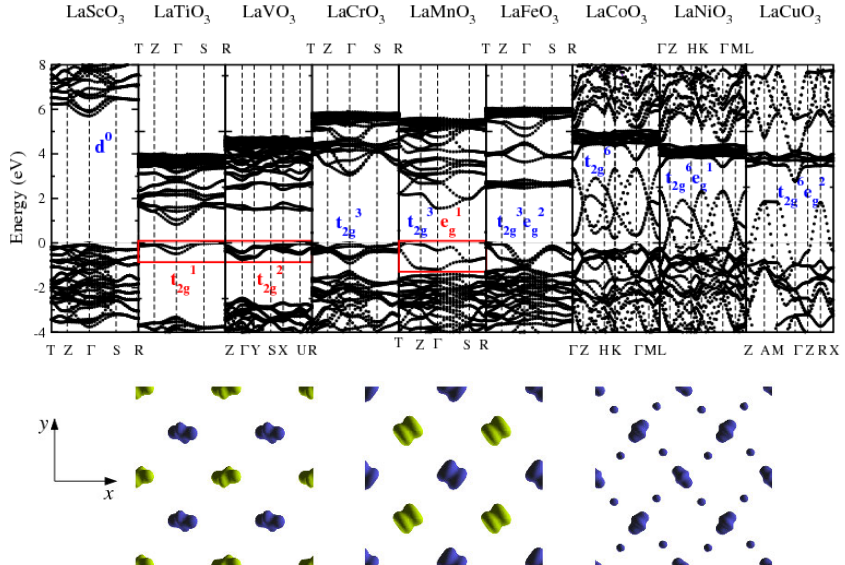
	LSO	LTO	LVO	LCrO	LaMO ₃	LFO	LaCoO	LNO	LaCuO
$\alpha_{opt}^{\text{HSE}}$	0.25	0.10/0.15	0.10-0.15	0.15	0.15	0.15	0.05	0	0
$\alpha_{opt}^{\epsilon_\infty}$ (ϵ_∞)	0.323 (3.1)	0.125 (8.0)	0.192 (5.2)	0.250 (4.0)	0.204 (4.9)	0.200 (5.0)	0.105 (9.5)	0 ∞	0 ∞

0.07 shift → HSE (screened) already contains some screening (μ)

Results: the 3d LaMO_3 perovskite dataset



Results: the 3d LaMO_3 perovskite dataset



Results: 4d and 5d perovskites

Larger spatial extension \Rightarrow Reduced correlation, Metallic & "itinerant magnetism"

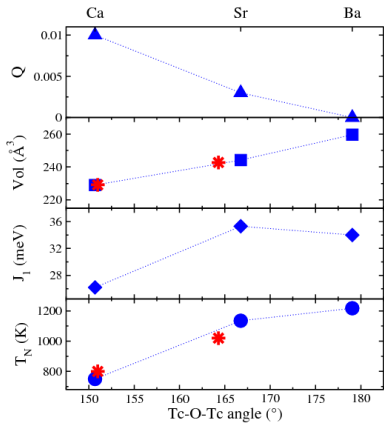
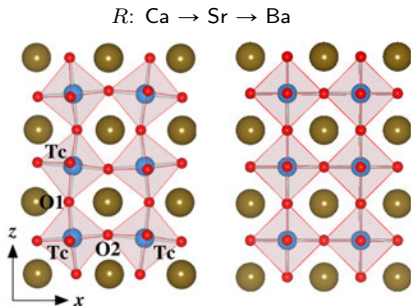
But...

25 Mn Manganese 54.938049	26 Fe Iron 55.845	27 Co Cobalt 58.933200
43 Tc Technetium (98)	44 Ru Ruthenium 101.07	45 Rh Rhodium 102.90550
75 Re Rhenium 186.207	76 Os Osmium 190.23	77 Ir Iridium 192.217

- High T_N in CaTcO_3 and SrTcO_3
M. Avdeedv *et al.*, JACS **133** 1654 (2011).
E.E. Rodriguez *et al.*, PRL **106** 067201 (2011).
- insulating state/weak magnetism in BaIrO_3
M.A. Laguna-Marco *et al.*, PRL **105** 216407 (2010).
R. Arita *et al.*, PRL **108**, 086403 (2012).
- Relativistic Mott state in Sr_2IrO_4
B.J. Kim *et al.*, PRL **101** 076402 (2008).
- Magnetic insulator NsOsO_3
Y. Shi *et al.* PRB **80**, 161104(R) (2009).

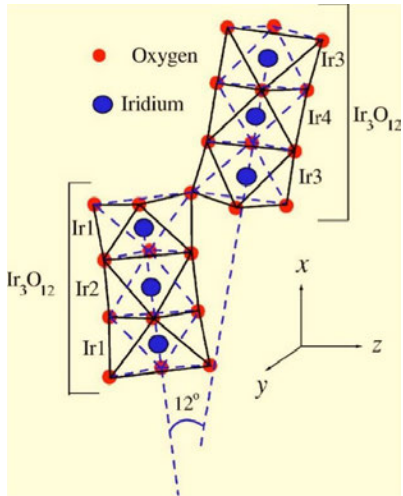
Results: 4d $RT\text{cO}_3$ perovskites

HSE total energies + $-\sum_{i < j} \mathbf{J}_{ij} \mathbf{S}_i \cdot \mathbf{S}_j$ + Monte Carlo



BaTcO₃: the highest T_N for compounds without 3d transition metals

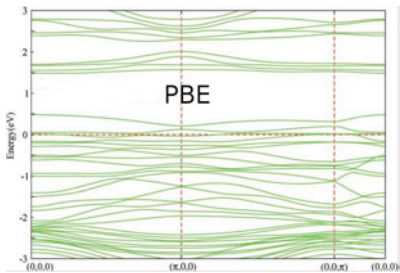
Results: 5d BaIrO₃ perovskite



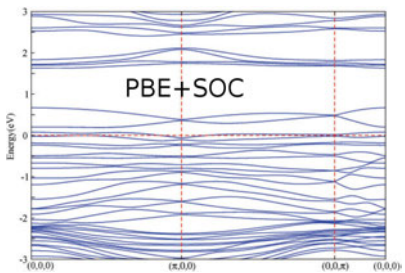
- Quasi 1D
- Weakly ferromagnetic $\mu \approx 0.03\mu_B$
- Nonmetallic (gap $\approx 10\text{-}50$ meV)
- Strong spin-orbit interaction

M. A. Laguna-Marco, et al., PRL 105, 216407 (2010).

Results: 5d BaIrO₃ perovskite



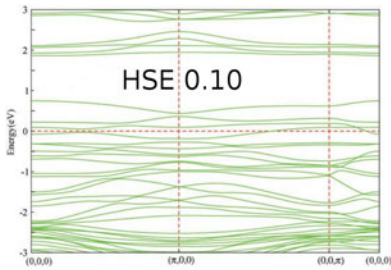
PBE



PBE+SOC

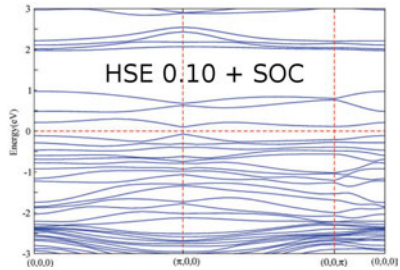
METAL !

Results: 5d BaIrO₃ perovskite



HSE 0.10

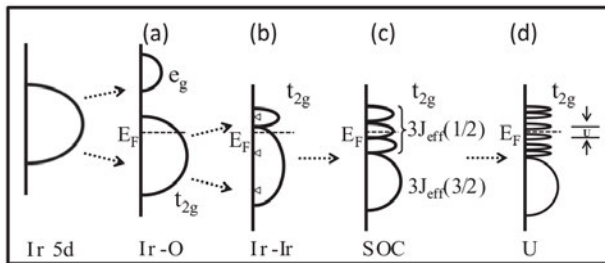
METAL !



HSE 0.10 + SOC

INSULATOR, $\mu \approx 0.1\mu_B$

Results: 5d BaIrO₃ perovskite



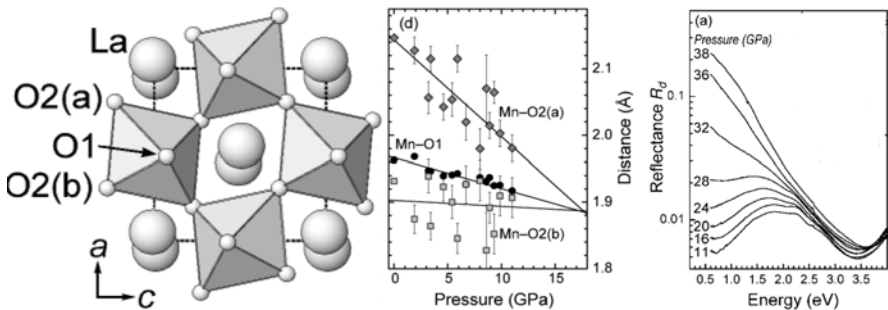
(a) Crystal field splitting: e_g , t_{2g}

(b) Ir-Ir interaction

(c) Spin-orbit coupling

(e) Moderate U

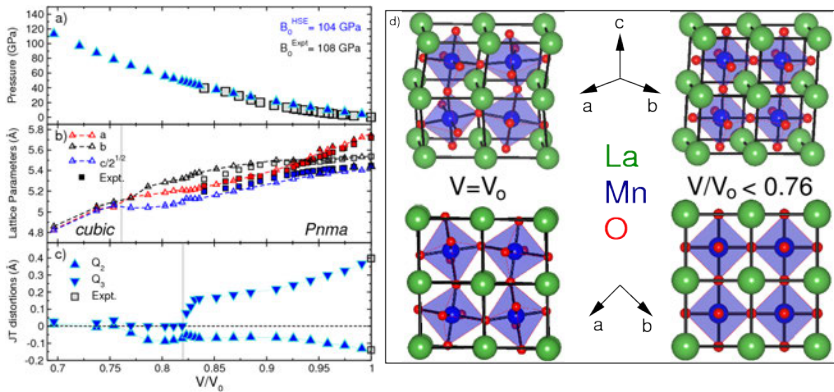
Results: MIT, LaMnO_3 under pressure



Loa *et al.* PRL 87, 125501 (2001)

- ① Progressive reduction of the JT distortions
- ② Insulator to metal transition (Mott ?, i.e. JT distortions in the insulating phase?)

Results: MIT, LaMnO₃ under pressure

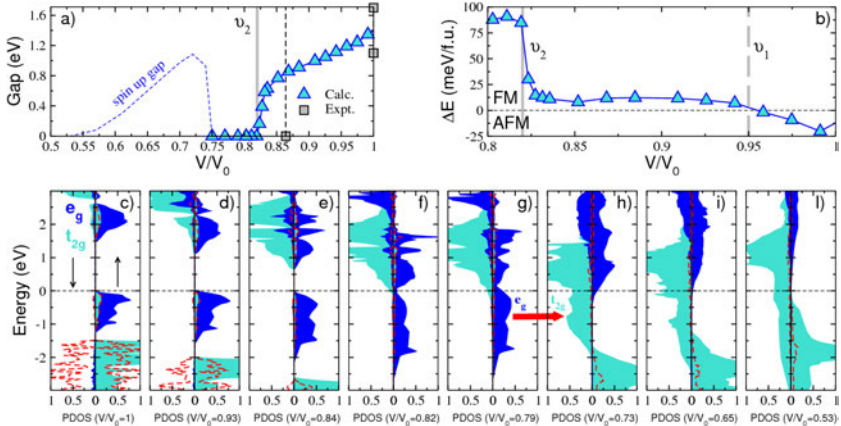


- ① Excellent agreement with Experiment

Loa *et al.* PRL **87**, 125501 (2001); L. Pinsard-Gaudart *et al.* PRB **64**, 064426 (2001)

- ② Progressive quenching of JT distortions
- ③ Orthorhombic to Cubic transition

Results: MIT, LaMnO₃ under pressure

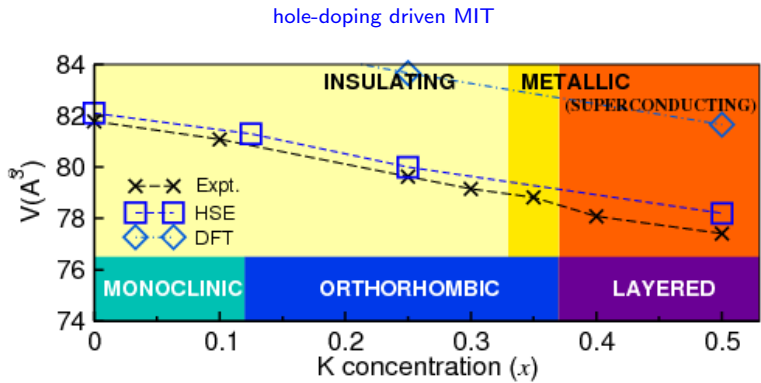


- ① $V/V_0=0.82 \Rightarrow$ non-Mott Insulator to metal transition

Trimarchi & Binggeli PRB 2005 (LDA+U); Yamasaki *et al.* PRL 2006 (DMFT)

- ② Intermediate pressure \Rightarrow AFM (distorted) FM (undistorted) competition
- ③ $V/V_0=0.70 \Rightarrow$ AFM to FM (& Low-spin to High spin) transition

Results: polarons in BaBiO₃

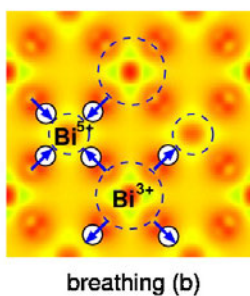
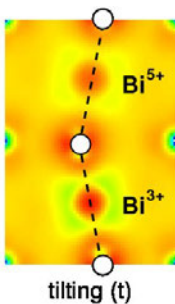
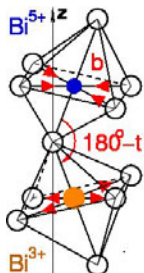


C. Franchini *et al.* PRL 102, 256402 (2009).
C. Franchini *et al.* PRB 81, 085213 (2010).

Results: polarons in BaBiO₃

x=0

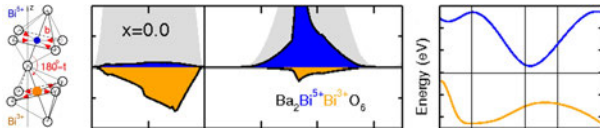
- Valence skipping \Rightarrow Charge disproportionation ($\text{Bi}^{4+} \Rightarrow \text{Bi}^{5+}/\text{Bi}^{3+}$, multivalency)
- Structural distortions \Rightarrow breathing (*b*) and tilting (*t*) instabilities
- Charged ordered (CDW) insulating state



Results: polarons in BaBiO₃

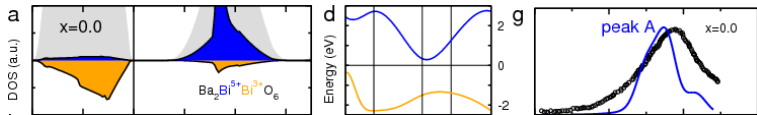
x=0

- Valence skipping \Rightarrow Charge disproportionation ($\text{Bi}^{4+} \Rightarrow \text{Bi}^{5+}/\text{Bi}^{3+}$, multivalency)
- Structural distortions \Rightarrow breathing (*b*) and tilting (*t*) instabilities
- Charged ordered (CDW) insulating state



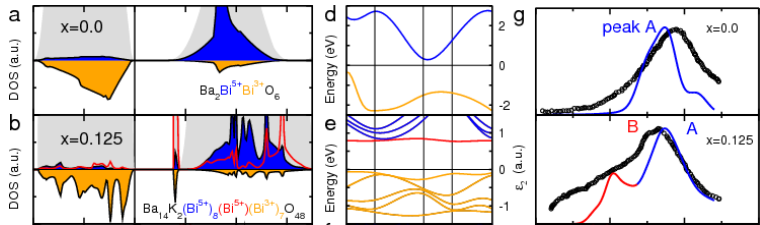
Results: polarons in BaBiO₃

$x > 0$



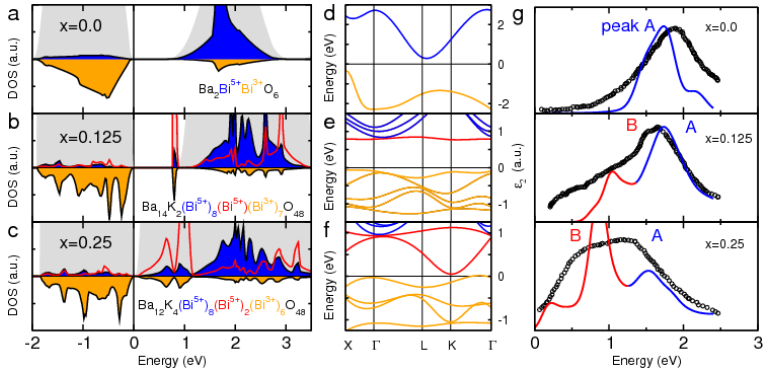
Results: polarons in BaBiO₃

$x > 0$



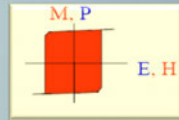
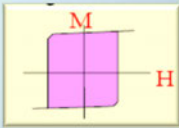
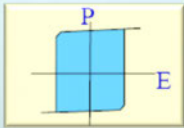
Results: polarons in BaBiO₃

$x > 0$



Results: Magnetism + Ferroelectricity

MULTIFERROICS



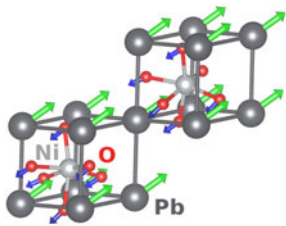
Ferroelectric Devices

Ferromagnetic Devices

Multiferroic Magnetoelectrics

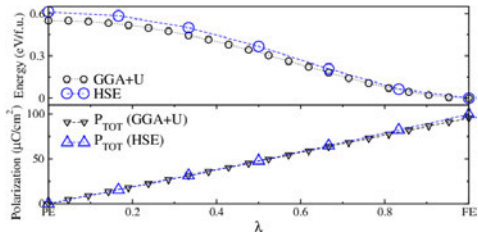
Results: Magnetism + Ferroelectricity

HSE + modern theory of polarization



LiNbO₃-type structure (*R*3c)

Arrows: FE displacements



Total polarization $\mathbf{P}_{\text{tot}} \sim 100 \mu\text{C}/\text{cm}^2$

Larger than BiFeO₃

Results: Crystal Structure Prediction

HSE + lattice dynamics + Group Theoretical Methods

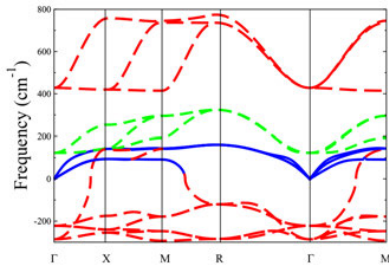
SrPdO₃: New perovskite created in 2010 (Journal of Power Sources **195** 3806)

Results: Crystal Structure Prediction

HSE + lattice dynamics + Group Theoretical Methods

SrPdO₃: New perovskite created in 2010 (Journal of Power Sources **195** 3806)

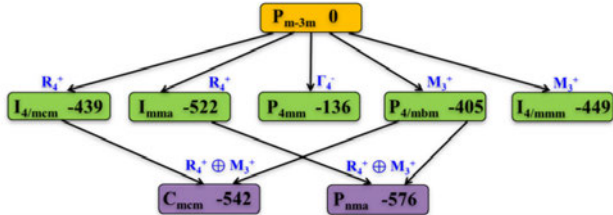
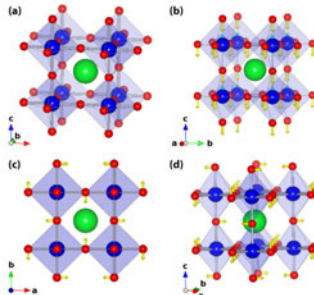
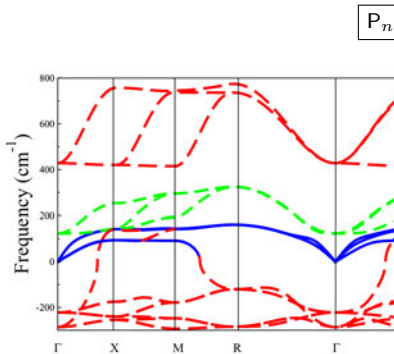
Structure: Unknown ($t=0.905 \rightarrow$ cubic phase unstable)



Strategy: stabilization of the negative modes (Γ_4^- , M_3^+ , R_4^+) through atomic displacements.

J. He & C. Franchini PRB 89, 045104 (2014).

Results: Crystal Structure Prediction



Summary

$$\left(-\frac{1}{2}\Delta + V_{\text{ext}}(\mathbf{r}) + V_{\text{H}}(\mathbf{r}) + \color{red}V_{\text{xc}}(\mathbf{r}) \right) \psi_{n\mathbf{k}}(\mathbf{r})$$

+

$$\left(-\frac{1}{2}\Delta + V_{\text{ext}}(\mathbf{r}) + V_{\text{H}}(\mathbf{r}) \right) \psi_{n\mathbf{k}}(\mathbf{r}) + \int \color{red}V_{\text{X}}(\mathbf{r}, \mathbf{r}') \psi_{n\mathbf{k}}(\mathbf{r}') d\mathbf{r}'$$

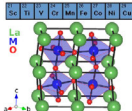
=

$$\left(-\frac{1}{2}\Delta + V_{\text{ext}}(\mathbf{r}) + V_{\text{H}}(\mathbf{r}) + V_{\text{c}}(\mathbf{r}) + \alpha V_{\text{x}}^{lr}(\mathbf{r}) + (1 - \alpha)V_{\text{x}}^{sr}(\mathbf{r}) \right) \psi_{n\mathbf{k}}(\mathbf{r}) + \int \color{red}\alpha V_{\text{x}}^{sr}(\mathbf{r}, \mathbf{r}') \psi_{n\mathbf{k}}(\mathbf{r}') d\mathbf{r}'$$

≈

$$\left(-\frac{1}{2}\Delta + V_{\text{ext}}(\mathbf{r}) + V_{\text{H}}(\mathbf{r}) \right) \psi_{n\mathbf{k}}(\mathbf{r}) + \int \color{red}\Sigma(\mathbf{r}, \mathbf{r}', E_{n\mathbf{k}}) \psi_{n\mathbf{k}}(\mathbf{r}') d\mathbf{r}'$$

Hybrid functionals for materials science: accurate and predictive



25 Mn Mn ₂ O ₃ (OH) ₂	26 Fe FexO	27 Co Co ₂ O ₃
43 7.00 Te TeO ₃ 180.207	44 7.00 Ru RuO ₃ 180.177	45 7.00 Rh Rh ₂ O ₃ 180.175
75 7.00 Os OsO ₃ 180.223	76 7.00 Ir IrO ₃ 180.175	

